In Vivo, High-Resolution, Three-Dimensional Imaging of Port Wine Stain Microvasculature in Human Skin

Gangjun Liu, PhD,[1,2] Wangcun Jia, PhD,[1] J. Stuart Nelson, MD, PhD,[1,2,3] and Zhongping Chen, PhD[1,2]*
[1]*Beckman Laser Institute and Medical Clinic, University of California, Irvine, California 92617*
[2]*Department of Biomedical Engineering, University of California, Irvine, California 92612*
[3]*Department of Surgery, University of California, Irvine, California 92697*

Background and Objectives: Port-wine stain (PWS) is a congenital, progressive vascular malformation of the dermis. The use of optical coherence tomography (OCT) for the characterization of blood vessels in PWS skin has been demonstrated by several groups. In the past few years, advances in OCT technology have greatly increased imaging speed. Sophisticated numerical algorithms have improved the sensitivity of Doppler OCT dramatically. These improvements have enabled the noninvasive, high-resolution, three-dimensional functional imaging of PWS skin. Here, we demonstrate high-resolution, three-dimensional, microvasculature imaging of PWS and normal skin using Doppler OCT technique.

Study Design/Materials and Methods: The OCT system uses a swept source laser which has a central wavelength of 1,310 nm, an A-line rate of 50 kHz and a total average power of 16 mW. The system uses a handheld imaging probe and has an axial resolution of 9.3 μm in air and a lateral resolution of approximately 15 μm. Images were acquired from PWS subjects at the Beckman Laser Institute and Medical Clinic. Microvasculature of the PWS skin and normal skin were obtained from the PWS subject.

Results: High-resolution, three-dimensional microvasculature of PWS and normal skin were obtained. Many enlarged PWS vessels are detected in the dermis down to 1.0 mm below the PWS skin surface. In one subject, the blood vessel diameters range from 40 to 90 μm at the epidermal–dermal junction and increase up to 300–500 μm at deeper regions 700–1,000 μm below skin surface. The blood vessels close to the epidermal–dermal junction are more uniform, in terms of diameter. The more tortuous and dilated PWS blood vessels are located at deeper regions 600–1,000 μm below the skin surface. In another subject example, the PWS skin blood vessels are dilated at very superficial layers at a depth less than 500 μm below the skin surface. The PWS skin vessel diameters range from 60 to 650 μm, with most vessels having a diameter of around 200 μm.

Conclusions: OCT can be used to quantitatively image in vivo skin micro-vasculature. Analysis of the PWS and normal skin blood vessels were performed and the results can provide quantitative information to optimize laser treatment on an individual patient basis. Lasers Surg. Med. © 2013 Wiley Periodicals, Inc.

Key words: medical optics and biotechnology; biology and medicine; optical coherence tomography; port sine stain

INTRODUCTION

Optical coherence tomography (OCT) is a noninvasive, noncontact technique, which provides a resolution of approximately 10 μm and a penetration depth of 2 mm. Port-wine stain (PWS) is a congenital, progressive vascular malformation of the dermis. The use of OCT for the characterization of blood vessels in PWS skin has been demonstrated by several groups, including our institution [1–4]. A time-domain OCT system has been used clinically for PWS imaging to determine epidermal thickness and the configuration of dilated capillary vessels from the analysis of two-dimensional OCT images [2]. As a functional extension of OCT, Doppler OCT has been demonstrated for noninvasive, two-dimensional imaging of blood vessels in PWS skin in situ and in real time [1]. In the past few years, advances in OCT technology have greatly increased imaging speed. Sophisticated numerical algorithms have improved the sensitivity of Doppler OCT dramatically [5]. These improvements have enabled noninvasive, high-resolution, three-dimensional functional imaging of PWS skin.

In this paper, we demonstrate high-resolution, three-dimensional microvasculature imaging of PWS and normal skin using a Doppler OCT technique. For in vivo,

G.L., W.J., and S.J.N. have no conflicts of interest. Z.C. is a co-found and the chairman of OCT Medical Imaging (OCTMI), Inc. Z.C has a financial interest in OCTMI, which, however, did not support this work.

Contract grant sponsor: National Institutes of Health; Contract grant numbers: AR59244, EB-10090, EY-021519, HL-105215, HL-103764, EB-015890; Contract grant sponsor: Air Force Office of Scientific Research; Contract grant number: FA9550-04-0101; Contract grant sponsor: Arnold and Mabel Beckman Foundation.

*Correspondence to: Zhongping Chen, PhD, Beckman Laser Institute and Medical Clinic, University of California, 1002 Health Sciences Road East, Irvine, CA 92612.
E-mail: z2chen@uci.edu

Accepted 1 October 2013
Published online in Wiley Online Library (wileyonlinelibrary.com).
DOI 10.1002/lsm.22194

awake patient imaging, involuntary movement by the subject will decrease image quality and introduce artifacts into the images. A frequency domain bandpass filter method is proposed to remove the sample movement induced artifacts in the en-face or maximum intensity projection (MIP) images. The microvasculatures of PWS and normal skin are compared.

MATERIALS AND METHODS

OCT System

An OCT system with a tunable micro-electro-mechanical systems (MEMS) optical filter based compact swept source laser was used in this study [6]. The laser has a central wavelength of 1,310 nm, an A-line rate of 50 kHz and a total average power of 16 mW (SSOCT-1310, Axsun Technologies, Inc., Billerica, MA). The FWHM bandwidth of the laser source was approximately 80 nm, resulting in a depth resolution of 9.3 μm in air. The OCT module adopted a Mach–Zehnder type interferometer with 90% and 10% of the laser light power in the sample and reference arms, respectively. The system utilized a K-trigger mode so that no linear wavenumber re-calibration was required. To facilitate subject imaging, a handheld probe was used which provided a lateral resolution of approximately 15 μm. The system was controlled by custom data acquisition software written in C++, running on a 64 bit Windows 7 operating system. The software is able to process and display the OCT images in real time and also has the capability to stream the acquired data onto a hard disk. The three-dimensional rendering and en-face images were performed offline using another custom software package written in C++. For PWS and normal skin vasculature imaging, several methods based on phase, intensity or both have been demonstrated [7]. In this manuscript, we will use the inter-frame intensity-based Doppler variance (IF-IBDV) method for the extraction of PWS and normal skin vasculature because of its simplicity and fast speed [6–8]. The measurement protocol has been approved by the Institutional Review Board at University of California, Irvine (Protocol #2010-7376). A total of 4096 B-scan frames with 1024 A-lines per frame will be acquired for the three-dimensional reconstruction. The three-dimensional data covers an area of 5 mm (length) × 5 mm (width) × 2.5 mm (height).

Involuntary Subject Movement Reduction

Involuntary subject movement during imaging is inevitable. Involuntary movement induced artifacts can greatly

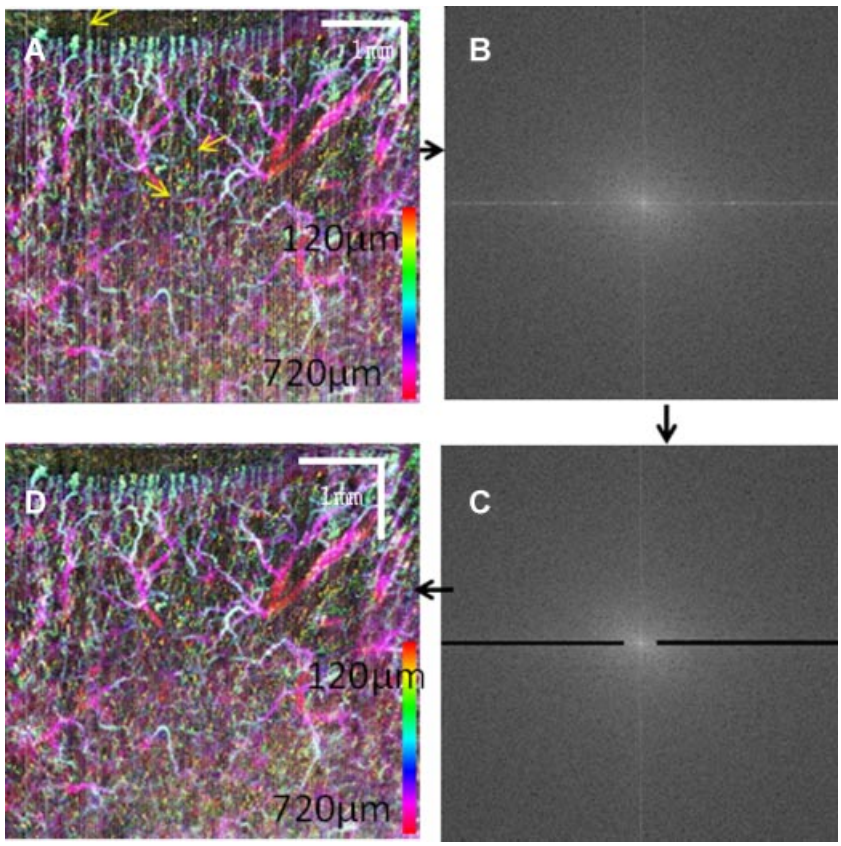

Fig. 1. Frequency domain bandpass filter method to reduce the sample movement induced artifacts. **A**: Color-coded, MIP *en-face* vasculature image of the dorsal finger region from a human volunteer. Yellow arrows point to vertical lines caused by the motion artifact. **B**: Fourier transform of (A). **C**: Bandpass filtering of (B). **D**: Inverse Fourier transform of (C).

degrade the image quality of the PWS and normal skin vasculature, particularly when the images are processed with phase-resolved methods [7]. Sophisticated numerical algorithms that statistically analyze the phase difference distribution may improve image quality and have been demonstrated by several groups [9,10]. Compared to phase-resolved methods, intensity-based methods are less sensitive to involuntary movement induced artifact [7,8]. However, such artifacts can still manifest themselves in the final vasculature images, particularly when inter-frame algorithms are used. In the final *en-face* or maximum intensity projection (MIP) *en-face* vasculature images, the artifact shows up as vertical or horizontal lines [11]. Structural image realignment using subpixel image registration has been used to eliminate these lines [11]. Although effective, this method greatly increases the computation time and complexity. Inasmuch as the artifact shows up as vertical or horizontal lines in the final *en-face* images, the artifact can be suppressed by processing the final *en-face* images. Here, a simple frequency domain filtering method is proposed to eliminate the artifact as shown in Figure 1. Figure 1A shows the color-coded, MIP *en-face* vasculature image of the dorsal finger region from a human volunteer. The motion artifact manifests itself as vertical lines as illustrated by the yellow arrows in the image. Figure 1B shows the two-dimensional Fourier transform of Figure 1A. In Figure 1C, a bandpass filter (black regions) is used in the Fourier domain image. The bandpass filter has a stopband between 0.1 and 1.0 (normalized frequency, where 1.0 corresponds to half the sampling frequency) in the horizontal direction and a stopband between 0 and 0.01 in the vertical direction. Figure 1D shows the inverse Fourier transform of Figure 1C. The effectiveness of this method can be seen by comparing Figure 1A and C. A vertical line in an image will show many horizontal lines in the Fourier domain with most of the energy concentrated around the zero frequency. By removing the energy from the zero frequency horizontal line in the Fourier domain, the vertical line in the original image will be eliminated. This simple method is suitable for removing vertical (or horizontal) lines artifacts in any image, which may be an OCT tomography image or an *en-face* image. Herein, the filter is applied to the final MIP *en-face* image and used only once. The method proposed here is fast and simple and the same filter may be used for different images. However, because this method filters the vertical (or horizontal) lines in the image, fine structure around the lines may be lost after filtering process.

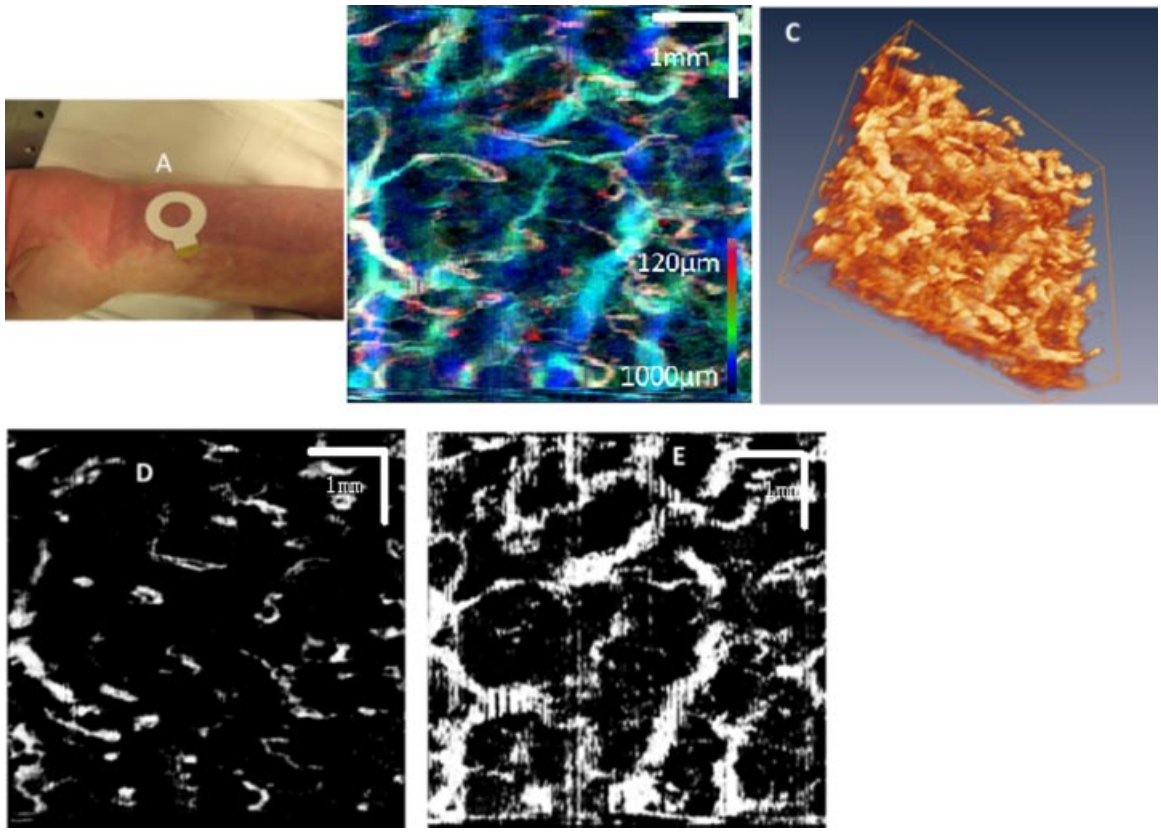

Fig. 2. **A**: Photograph shows the imaging location (area enclosed by white circle) on a subject's PWS. **B**: The MIP images of the PWS skin microvasculature. **C**: 3D rendering of the PWS skin microvasculature (movie). **D**: PWS skin microvasculature at a layer close to the epidermal–dermal junction. **E**: PWS skin microvasculature at a depth approximately 800 μm below the skin surface.

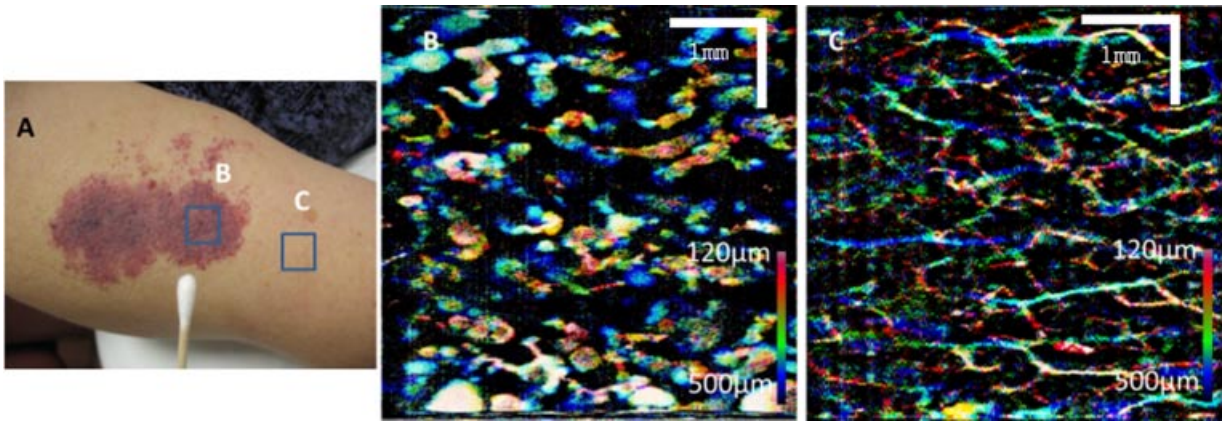

Fig. 3. **A**: Photograph showing the imaging locations (areas enclosed by blue squares) on a subject's PWS. **B**: The MIP image of the PWS skin microvasculature. **C**: The MIP image of the normal skin microvasculature.

RESULTS

The three-dimensional vasculature of PWS skin was imaged using OCT. The subject is a 40-year-old male and the PWS area imaged with OCT has not been previously treated by laser. The PWS has a dark-red to purple color and there is no hypertrophy or nodularity. In Figure 2, the photograph shows the location imaged by OCT (area enclosed by white circle) on the subject's PWS. Figure 2B is the MIP image of the PWS skin microvasculature. Figure 2C shows a three-dimensional rendering of the PWS skin microvasculature. Figure 2D shows PWS skin microvasculature at a layer close to the epidermal–dermal junction. Figure 2E shows PWS skin microvasculature at a depth approximately 800 μm below the skin surface.

Figure 3 shows the photograph and OCT imaging of another PWS lesion. In this subject example, the PWS is located on the upper arm of a female subject. The PWS region is purple in color, as shown in Figure 3A. The entire PWS has not been previously treated by laser and small black nodules can be seen on the skin surface of the lesion. Figure 3B and C shows the PWS and normal skin microvasculature images, respectively.

DISCUSSION

Three-dimensional imaging of the subsurface vessel network can provide information for accurate PWS classification and guidance for effective treatment. Invasive methods such as histology following biopsy and confocal microscopy have been used to determine PWS blood vessel geometry in human skin [12,13]. However, in situ diagnostic knowledge of PWS blood vessel characteristics, such as mean depth and diameter, are always preferred to help provide guidance on the selection of the optimal laser treatment parameters on an individual patient basis for effective PWS treatment.

In the case shown in Figure 2, many enlarged PWS vessels are detected in the dermis down to 1.0 mm below the skin surface. The Figure 2B and C provide a realistic three-dimensional representation of the PWS vessel geometry. The blood vessel diameters range from 40 to 90 μm at the epidermal–dermal junction and increase up to 300–500 μm at deeper regions 700–1,000 μm below skin surface. In this PWS subject, the blood vessels close to the epidermal–dermal junction are more uniform, in terms of diameter, as shown in Figure 2D. The more tortuous and dilated PWS blood vessels are located at deeper regions 600–1,000 μm below the skin surface, as shown in Figure 2E.

In the case shown in Figure 3, the PWS skin blood vessels are dilated at very superficial layers at a depth less than 500 μm below the skin surface. The PWS skin vessel diameters range from 60 to 650 μm, with most vessels having a diameter of around 200 μm. A few very large dilated tortuous blood vessels shown in Figure 3(B) may be clusters of small vessels, whose diameters are beyond the resolution of our current OCT system [13]. The normal skin blood vessel diameters are less than 90 μm.

CONCLUSIONS

In conclusion, herein we have demonstrated noninvasive, high-resolution, three-dimensional, microvasculature imaging of PWS and normal skin using a Doppler OCT technique. Analysis of the PWS and normal skin blood vessel were performed and the results can provide quantitative information to optimize laser treatment on an individual patient basis. A frequency domain bandpass filter method was proposed to reduce the sample movement induced artifacts during in vivo awake patient imaging.

ACKNOWLEDGEMENTS

This work was supported by the National Institutes of Health (AR59244, EB-10090, EY-021519, HL-105215, HL-103764, and EB-015890), the Air Force Office of Scientific Research (FA9550-04-0101), and the Arnold and Mabel Beckman Foundation. Dr. Chen has a financial interest in

OCT Medical Imaging Inc., which, however, did not support this work.

REFERENCES

1. Nelson JS, Kelly KM, Zhao Y, Chen Z. Imaging blood flow in human port-wine stain in situ and in real time using optical Doppler tomography. Arch Dermatol 2001; 137:741.
2. Shiyong Z, Ying G, Ping X, Jin G, Tingme IS, Tianshi E, Naiyan H, Li Z, Haixia Q, Xin Y, Xunbin W. Imaging port wine stains by fiber optical coherence tomography. J Biomed Opt 2010;15:036020. doi: 10.1117/1.3445712
3. Zhao Y, Chen Z, Ding Z, Ren H, Nelson JS. Three-dimensional reconstruction of in vivo blood vessels in human skin using phase-resolved optical Doppler tomography. IEEE J. Selected Top Quantum Electron 2001;7:931.
4. Zhou Y, Yin D, Xue P, Huang N, Qiu H, Wang Y, Zeng J, Ding Z, Gu Y. Imaging of skin microvessels with optical coherence tomography: Potential uses in port wine stains. Exp Ther Med 2012;4:1017.
5. Liu G, Chen Z. Advances in Doppler OCT. Chin Opt Lett 2013;11:011792.
6. Liu G, Jia W, Sun V, Choi B, Chen Z. High-resolution imaging of microvasculature in human skin in-vivo with optical coherence tomography. Opt Express 2012;20:7694.
7. Liu G, Lin AJ, Tromberg BJ, Chen Z. A comparison of Doppler optical coherence tomography methods. Biomed Opt Express 2012;3:2669.
8. Liu G, Chou L, Jia W, Qi W, Choi B, Chen Z. Intensity-based modified Doppler variance algorithm: Application to phase instable and phase stable optical coherence tomography systems. Opt Express 2011;19:11429.
9. Yang VX, Gordon ML, Mok A, Zhao Y, Chen Z, Cobbold RSC, Wilson BC, Vitkin IA. Improved phase-resolved optical Doppler tomography using the Kasai velocity estimator and histogram segmentation. Opt Commun 2002;208:209.
10. Makita S, Hong Y, Yamanari M, Yatagai T, Yasuno Y. Optical coherence angiography. Opt Express 2006;14:7821.
11. Lee KKC, Mariampillai A, Yu JXZ, Cadotte DW, Wilson BC, Standish BA, Yang VXD. Real-time speckle variance swept-source optical coherence tomography using a graphics processing unit. Biomed Opt Express 2012;3:1557.
12. Smithies D, van Gemert M, Hansen M, Milner T, Nelson J. Three-dimensional reconstruction of port wine stain vascular anatomy from serial histological sections. Phys Med Biol 1997;42:1843.
13. Selim MM, Kelly KM, Nelson JS, Wendelschafer-Crabb G, Kennedy WR, Zelickson BD. Confocal microscopy study of nerves and blood vessels in untreated and treated port-wine stains: Preliminary observations. Dermatol Surg 2004;30: 892–897.